Spatial Variability in In Situ Aerobic Respiration and Denitrification Rates in a Petroleum-Contaminated Aquifer

by M.H. Schroth[a], J.D. Istok[a], G.T. Conner[a], M.R. Hyman[b], R. Haggerty[c], and K.T. O'Reilly[d]

Abstract

An extensive series of single-well, push-pull tests was performed to quantify horizontal and vertical spatial variability in aerobic respiration and denitrification rates in a petroleum-contaminated aquifer. The results indicated rapid consumption of injected O_2 or NO_3^- in shallow and deep test intervals across a large portion of the site. Computed first-order rate coefficients for aerobic respiration ranged from 0.15 to 1.69 h^{-1} in the shallow test interval, and from 0.08 to 0.83 h^{-1} in the deep test interval. The largest aerobic respiration rates occurred on the upgradient edge of the contaminant plume where concentrations of petroleum hydrocarbons and dissolved O_2 were relatively high. Computed first-order rate coefficients for denitrification ranged from 0.09 to 0.42 h^{-1} in the shallow test interval, and from 0.11 to 0.28 h^{-1} in the deep test interval. The largest denitrification rates occurred on the downgradient edge of the plume where hydrocarbon concentrations were relatively high but dissolved oxygen concentrations were small. The rates reported here represent maximal rates of aerobic respiration and denitrification, as supported by high concentrations of electron acceptors in the injected test solutions. Production of dissolved CO_2 during aerobic respiration and denitrification tests provided evidence that O_2 and NO_3^- consumption was largely due to microbial activity. Additional evidence for microbial NO_3^- consumption was provided by reduced rates of NO_3^- consumption when dissolved O_2 was injected with NO_3^-, and by increased N_2O production when C_2H_2 was injected with NO_3^-.

Introduction

Quantitative information on subsurface microbial metabolic activities is needed (1) to improve our understanding of microbiological processes in pristine and contaminated environments; (2) to predict rates of natural microbial attenuation of contaminants; and (3) to evaluate the effectiveness of microbial-based treatment technologies. Microorganisms display a broad metabolic diversity but share the ability to obtain energy for cell production and maintenance by facilitating oxidation-reduction reactions. A wide variety of compounds may serve as electron donors and these may be either organic or inorganic; substantially fewer compounds may serve as electron acceptors and these are most commonly inorganic (Brock and Madigan 1991). It is often possible to use observed changes in electron acceptor concentrations as quantitative indicators of microbial activity (e.g., Thorstenson et al. 1979). This concept is especially applicable in contaminated environments, where microbial activity is typically limited by the availability of suitable electron acceptors (McAllister and Chiang 1994).

Aerobic respiration, in which O_2 is the electron acceptor, is the most energetically favorable form of respiration (Jorgensen 1989). In the absence of O_2, a variety of anaerobic respiration and fermentation processes may occur (Ghiorse and Wilson 1988). The most energetically favorable anaerobic respiration process is denitrification, wherein the oxidation of inorganic or organic carbon is coupled to the reduction of NO_3^- (Brock and Madigan 1991).

In contaminated environments, we expect microbial metabolic activity to vary both spatially and temporally in response to variations in types and concentrations of available electron donors and/or electron acceptors (Smith et al. 1991). For example, Federle et al. (1990) reported rapid decreases in microbial biomass and activity with depth in an aquifer contaminated by infiltrating waste water. Ronen et al. (1987) and Cozzarelli et al. (1988) reported high rates of aerobic respiration near the water table, while rates of anaerobic activity increased with increasing depth below the water table. Harvey et al. (1984) and Chiang et al. (1989) reported steep horizontal gradients in dissolved O_2 across the perimeter of contaminant plumes and attributed this to the occurrence of high rates of aerobic respiration in these locations.

A wide variety of laboratory-based methods have been used to estimate subsurface microbial metabolic activities including microcosms (Wilson et al. 1983), direct observation (Harvey et al. 1984), biochemical markers (Balkwill et al. 1988), molecular methods (Bowman et al. 1993), analysis of geochemistry data (Lovley and Goodwin 1988), and ecological modeling (Kelly et al. 1988).

[a]Department of Civil, Construction and Environmental Engineering, Oregon State University, Corvallis, OR 97331, (541) 737-2695 [voice], (541) 737-3099 [fax]. E-mail: schrothm@ucs.orst.edu (first author).

[b]Department of Botany and Plant Pathology, Oregon State University, Corvallis, OR 97331.

[c]Department of Geosciences, Oregon State University, Corvallis, OR 97331

[d]Chevron Research and Technology Co., 100 Chevron Way, Richmond, CA 94802.

Received March 1997, accepted February 1998.

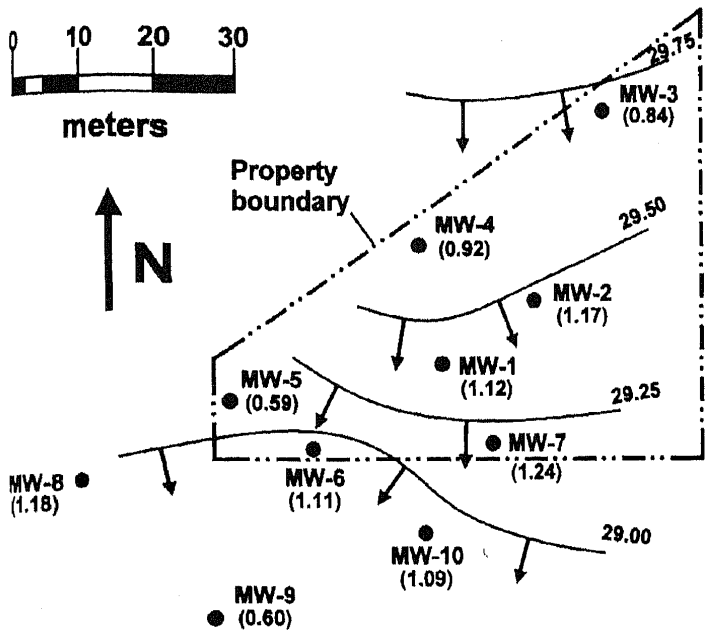

Figure 1. Site map showing monitoring well locations, water table elevation contours (meters above sea level), inferred ground water flow direction (arrows), and water table depths in meters (inside parentheses).

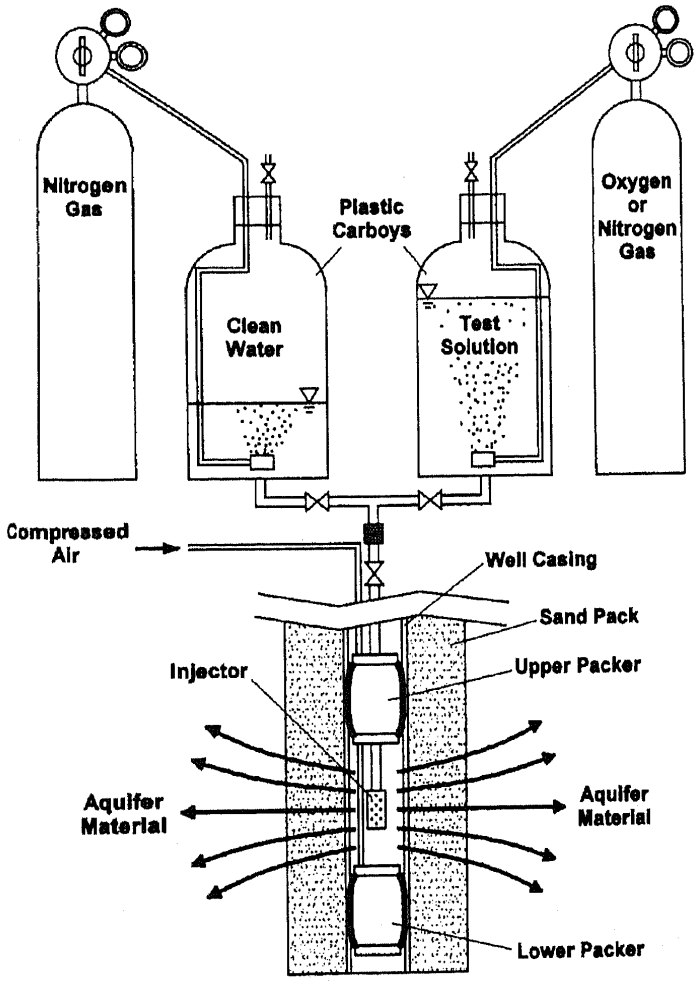

Figure 2. Equipment used during the injection phase of field push-pull tests (not to scale).

However, it is becoming increasingly apparent that in situ testing methods (e.g., Trudell et al. 1986; Gillham et al. 1990; Istok et al. 1997) will be required to describe the spatial variability in microbial metabolic activity, especially in the deep subsurface and in contaminated environments (Madsen 1991). As these methods have not been widely used, only a limited amount of data are currently available to help establish spatial relationships between microbial metabolic activities and concentrations of various electron donors and acceptors in contaminated environments.

The objectives of this study were to quantify the spatial variability in potential rates of aerobic respiration and denitrification in a petroleum-contaminated aquifer; and to examine the spatial relationships between these rates and concentrations of potential electron donors, electron acceptors, and metabolic products at the site. Aerobic respiration and denitrification were selected because they play an important role in both intrinsic bioremediation and enhanced bioremediation strategies (Madsen 1991). Rates were measured in situ using the recently developed single-well, push-pull test method (Istok et al. 1997). Because the microbial activities we determined are based on measured rates of consumption of injected O_2 or NO_3^-, an important component of this study was to determine whether the observed consumption rates were attributable to microbial activity or to abiotic processes.

Methods

Site Description

The study area was a former gasoline/diesel fuel distribution terminal in Newberg, Oregon. A portion of the site was contaminated with petroleum hydrocarbons from leaking storage tanks and surface spills which occurred between the 1930s and 1991. The storage tanks were removed between 1991 and 1993 but no other remediation actions were taken. Ten monitoring wells were installed between 1991 and 1995 (Figure 1). Wells were constructed of 5.1 cm I.D. polyvinyl chloride casing and screen and were installed inside an 11 or 15 cm hole created with a hollow stem auger to a depth of between 5 and 7 m below ground surface. The wells were screened across the entire saturated thickness of the aquifer. The annular space of each well was filled with clean sand, except near the surface, where bentonite and concrete were used to seal the annular space. Boring logs indicate that the aquifer consists primarily of lacustrine deposits of clayey silt and silt, with occasional traces of fine sand, gravel, and peat. The aquifer is unconfined and water table depths ranged from 0.59 to 1.24 m (Figure 1). Regional ground water flow is generally from north to south; the hydraulic gradient is approximately 0.01 m/m, and the average ground water (Darcy) velocity is approximately 10^{-3} m/d.

Push-Pull Test Procedures

Two vertically separated inflatable rubber packers were used to isolate 1 m long test intervals within the screened portion of the wells (Figure 2). Tests were performed at two depths in each well, designated as "shallow" and "deep." For the shallow tests, a 10 cm long injector was placed approximately 1.5 m below the water table; for the deep tests, the injector was placed approximately 4.5 m below the water table.

Prior to conducting push-pull tests at the site, ground water samples were collected from all test intervals and analyzed to determine initial background concentrations of total organic carbon (TOC), total petroleum hydrocarbons gasoline (C_6 through C_{10}, TPH-G), benzene, toluene, ethyl benzene, and xylene isomers (BTEX), dissolved O_2, NO_3^-, NO_2^-, SO_4^{2-}, Fe(II), dissolved CO_2, and pH. All test intervals were purged before collecting ground water samples by pumping at least 30 L of ground water (approximately three times the estimated volume of water within the well casing and sand pack between the two packers) using a peristaltic pump (Barnant Model E1188, Cole-Parmer, Niles, Illinois).

Test and clean water solutions were prepared from tap water in 50 L plastic carboys (Figure 2). For aerobic respiration tests, the test solution contained 100 mg/L Br^-, prepared from KBr, and a dissolved O_2 concentration between 33 and 47 mg/L, prepared by bubbling O_2 gas through the test solution prior to injection. For denitrification tests, the test solution contained 100 mg/L Br^-, a dissolved O_2 concentration < 0.5 mg/L, prepared by bubbling N_2 gas through the test solution prior to injection, and 25 mg/L NO_3^--N prepared from $NaNO_3$. The clean water flushing solution contained no Br^- and had a dissolved O_2 concentration < 0.5 mg/L.

Before each test, the test interval was purged and ground water was analyzed for Br^-, dissolved CO_2, and dissolved O_2 or NO_3^-. Then ~ 30 L of test solution were injected followed by the injection of 10 L of clean water (both at ~ 1 L/min) to flush the test solution from the well casing and sand pack into the aquifer. The volume of test solution and clean water combined represents the volume of water required to penetrate into the aquifer a radial distance of ~ 15 cm beyond the outer edge of the sand pack (Istok et al. 1997).

The extraction phase began immediately after the end of the injection phase using a peristaltic pump. The pump effluent was first passed through a flow-through cell which provided temperature stability for the O_2 electrode used to measure dissolved O_2, and then collected in volumetric containers. Samples for Br^-, dissolved CO_2, and dissolved O_2 or NO_3^- were collected every 2 L during the extraction phase of the tests. Extraction phase pumping (at ~ 1 L/min) continued until Br^- concentrations were reduced to background levels, which typically required an extraction volume of between 50 and 60 L.

Verification of Microbial Metabolic Activity

Following the completion of all tests described in the previous section, a limited number of additional push-pull tests were performed in selected test intervals and wells in an attempt to verify that observed O_2 and NO_3^- consumption was due to microbial activity and not abiological chemical reactions (e.g., O_2 or NO_3^- reduction by Fe(II)). In one type of test, a portion of the aquifer was treated to reduce numbers of living organisms by injecting approximately 30 L of a 2% solution of sodium hypochlorite. After allowing the solution to react with the aquifer for approximately 48 hours, an aerobic respiration test was performed in the treated zone using the identical methods described previously. In another type of test, denitrification tests were performed using test solutions that contained between 43 and 46 mg/L dissolved O_2 (in addition to Br^- and NO_3^-) to inhibit the activity of anaerobic denitrifying bacteria. In yet another type of test, denitrification tests were performed using solutions containing Br^- and NO_3^- that were saturated with a mixture of 10% acetylene (C_2H_2) gas in N_2 to block N_2 gas production from N_2O. This is an application of the "acetylene block" technique that has been widely used to verify denitrifying activity in microcosm studies (e.g., Balderston et al. 1976; Yoshinari and Knowles 1976). During the extraction phase of these tests, water samples were collected for C_2H_2 and nitrous oxide (N_2O) analyses by injecting 10 mL of water into 40 mL glass serum bottles capped with rubber septa.

Analytical Methods

Analyses for nonvolatile TOC, hereafter referred to as TOC, were performed using a TOC analyzer (Model Dohrman DC-190, Rosemount Analytical, Santa Clara, California) by separately measuring total carbon (TC) and inorganic carbon (IC) to obtain TOC as the difference between TC and IC (method 5310; APHA et al. 1992). Samples were analyzed for TPH-G using OR-TPH-G (ODEQ 1990) and for BTEX using EPA method 8020 (U.S. EPA 1986).

Bromide concentrations were measured using a combination glass body Br^- electrode (Model 27502-05, Cole Parmer Instrument Co., Niles, Illinois) and ion-specific meter (Accumet Model 25, Denver Instrument Co., Arvada, Colorado). Dissolved O_2 concentrations were determined with either a colorimetric assay based on Rhodazine D reduction (CHEMetrics Inc., Calverton, Virginia) for O_2 concentrations ≤ 1 mg/L, or with a Clark-type polarigraphic probe and meter (Models 5331 and 5300, Yellow Springs Instrument Co., Yellow Springs, Ohio) for O_2 concentrations >1 mg/L. Nitrate concentrations were determined by a colorimetric assay based on cadmium reduction and organic dye formation (CHEMetrics Inc., and HACH Co., Loveland, Colorado). Sulfate concentrations were determined by reacting $BaCl_2$ with the sample to form a $BaSO_4$ precipitate and measuring the resulting turbidity with a colorimeter (Model DR/700, HACH Co.). A colorimetric analysis based on the use of an acidic, buffered solution of 1,10-phenanthroline (CHEMetrics Inc.) was used to measure Fe(II) concentrations.

Dissolved CO_2 concentrations were determined by a titration/colorimetric assay (CHEMetrics Inc.), in which a caustic titrant was titrated with sample until the phenolphthalein end point (pH = 8.3) was reached (method 4500-CO_2 C; APHA et al. 1992). This method was employed despite the presence of Fe(II) in concentrations > 1.0 mg/L. Noting that no precipitates formed during the assays, the magnitude of Fe(II) interference on measured CO_2 concentrations was estimated from the reaction: $Fe(II) + H_2O \leftrightarrow FeOH^+ + H^+$; $\log K = -9.5$ (at 25°C; Stumm and Morgan 1981). At pH = 8.3, only ~ 5% of all Fe(II) in solution is in the form of $FeOH^+$. Given the concentration ratios of Fe(II) / CO_2 at our site (Table 1), we found that the largest relative error in measured CO_2 concentrations due to Fe(II) interference is ~ 1%, which we considered insignificant.

Ground water pH was measured using an Oakton Meter (Fisher Scientific, Pittsburgh, Pennsylvania). Dissolved C_2H_2 concentrations were analyzed using a gas chromatograph (Model 3700 Varian Corp., Walnut Creek, California) equipped with a flame ionization detector. Dissolved N_2O concentrations were analyzed using the same gas chromatograph equipped with an electron capture detector and a 1.5 m stainless steel column containing Porapak R. The column and detector temperatures were 35 and 320°C, respectively, and the carrier gas was 5% CH_4 in Ar.

Data Analysis

The total masses of injected Br^- and dissolved O_2 or NO_3^- were computed for each test from the known solute concentrations and measured volumes of injected test solutions. Similarly, the total masses of extracted Br^- and dissolved O_2 or NO_3^- were computed by integrating measured solute concentrations and extraction volumes during the extraction phase.

Rate coefficients of injected O_2 or NO_3^- consumption were determined using the method of Haggerty et al. (1998), which is based on an analysis of injected tracer and reactive solute transport in the alternating diverging/converging radial flow field surrounding a monitoring well during a push-pull test. Their approach assumes that an injected reactive solute is transformed within the aquifer according to the "first-order" type reaction $\partial C_r/\partial t = -k C_r$

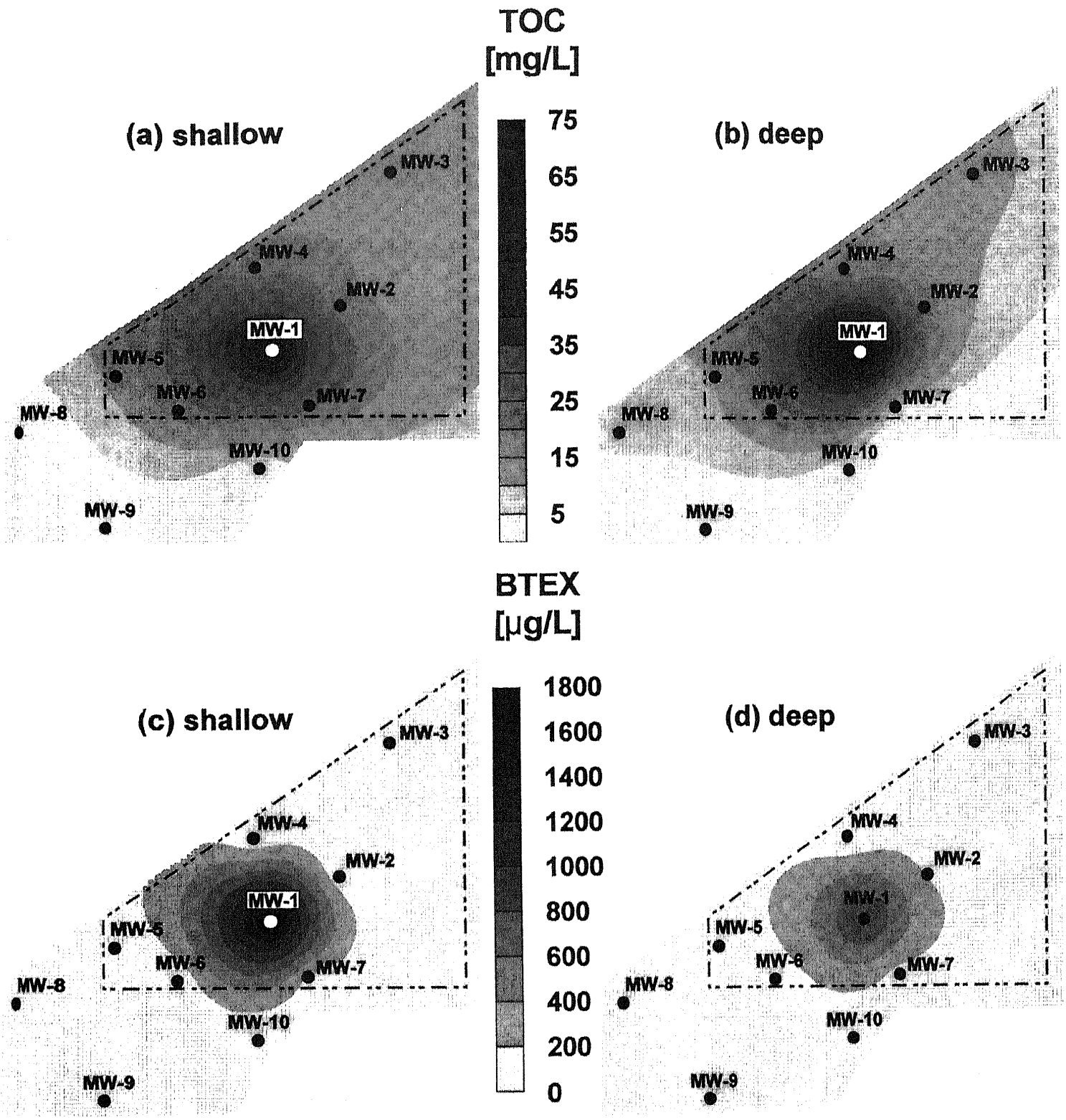

Figure 3. **Spatial variability in initial background concentrations of TOC (a and b), and BTEX (c and d) in shallow and deep test intervals.**

so that

$$C_r(t) = C_r^o e^{-kt} \quad (1)$$

where $C_r(t)$ is the reactive solute concentration at time t, C_r^o is the reactive solute concentration at time $t = 0$, and k $[T^{-1}]$ is the rate coefficient. Their approach also assumes that the injected test solution is well mixed with ground water within the aquifer, that the advection-dispersion transport properties of tracer and reactant are identical, and that changes in saturated thickness due to injection and extraction pumping are negligible. With these assumptions, the breakthrough curve for a reactive solute $C_r(t^*)$ is given by

$$C_r(t^*) = \frac{C_{tr}(t^*)}{k\, t_{inj}} \left[e^{-kt^*} - e^{-k(t_{inj}+t^*)} \right] \quad (2)$$

where t^* is the time elapsed since the end of the test solution injection, $C_{tr}(t^*)$ is the breakthrough curve for a co-injected tracer, and t_{inj} is the duration of the test solution injection. Equation 2 can be rewritten:

$$\ln\left(\frac{C_r(t^*)}{C_{tr}(t^*)}\right) = \ln\left[\frac{(1 - e^{-kt_{inj}})}{k\, t_{inj}}\right] - k\, t^* \quad (3)$$

so that a plot of $\ln (C_r/C_{tr})$ versus t^* generates a straight line with

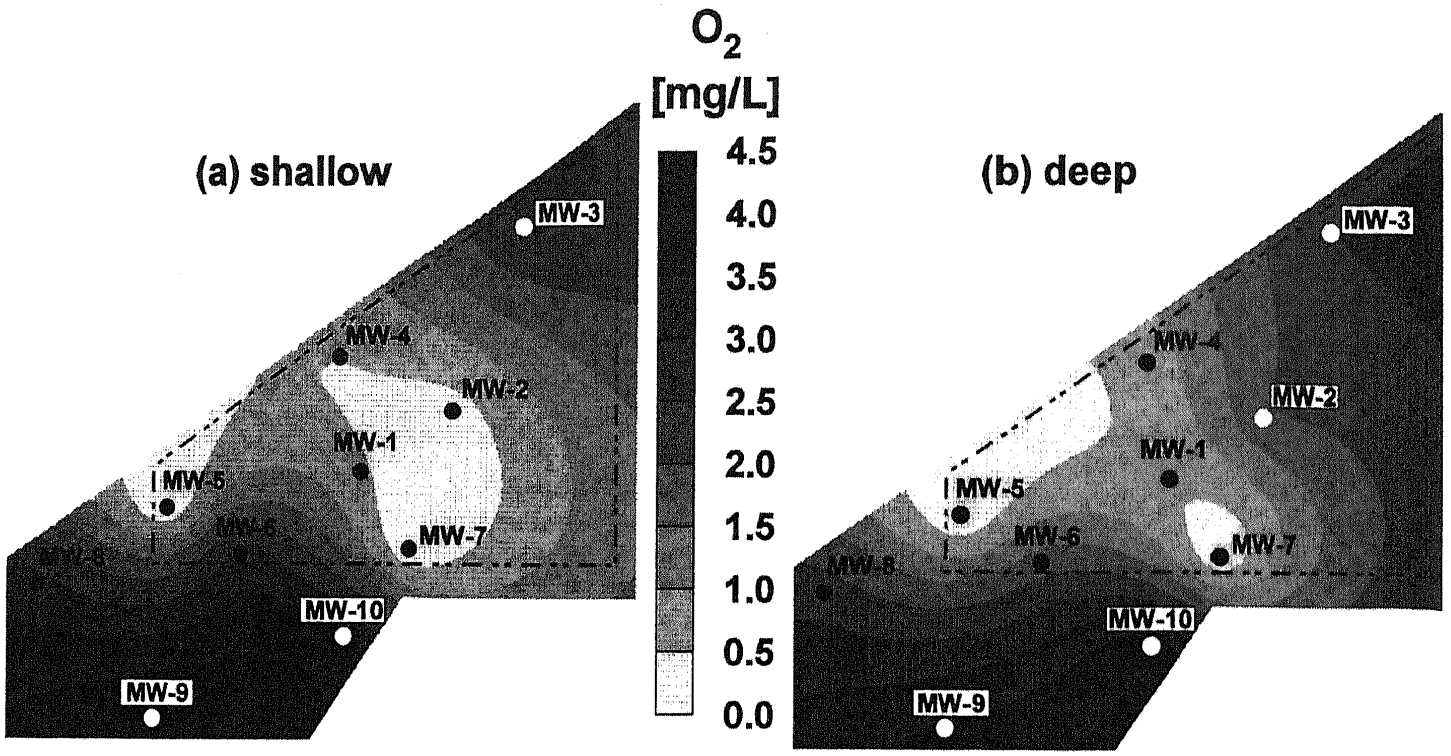

Figure 4. Spatial variability in initial background concentrations of dissolved O_2 in (a) shallow and (b) deep test intervals.

a slope $-k$ and intercept ln $[(1-e^{-k\,t_{inj}})/\,k\,t_{inj})]$. Haggerty et al. (1998) showed that fitting Equation 3 to push-pull test breakthrough curves gives accurate estimates for k for a wide range of aquifer properties and test conditions including both homogeneous and heterogeneous patterns of hydraulic conductivity.

Since the determination of k is based on the evaluation of ratios of C_r/C_{tr} as a function of t* (Equation 3), no complete tracer mass recovery is required during push-pull tests to obtain accurate estimates of k. Note that this differs from the frequently used method of moments to determine k (e.g., Istok et al. 1997), in which a high tracer mass recovery is required to obtain accurate estimates of k. A nonlinear least-squares routine was used to fit Equation 3 (both slope and intercept) to experimental breakthrough data to obtain estimates for first-order rate coefficients for aerobic respiration and denitrification for each test interval and well. For this purpose, C_r in Equation 3 is the relative concentration (i.e., the measured concentration divided by the known concentration in the injected test solution) of either O_2 (aerobic respiration tests) or NO_3^- (denitrification tests) and C_{tr} is the relative concentration of Br^- (both types of test). Additional details and example calculations are in Haggerty et al. (1998).

To determine the 95% confidence intervals for the estimated k, we assumed (1) that changes in ln (C_r/C_{tr}) are approximately linear with respect to changes in k in Equation 3 in the region of the parameter estimate; and (2) the errors in ln (C_r/C_{tr}) are normally distributed and have the same distribution through time. For this case, a first-order estimate of the parameter covariance matrix, $\mathbf{V}_p$ is given by (after Bard 1974; Draper and Smith 1981):

$$\mathbf{V}_p = \sigma^2(\mathbf{J}^T\mathbf{J})^{-1} \tag{4}$$

where σ^2 [-] is the variance of the errors in ln (C_r/C_{tr}) and $\mathbf{J}$ is the Jacobian matrix. Since we estimate only one parameter (i.e., k), $\mathbf{J}$ is simply the vector of the first derivative of Equation 3 with respect to k, evaluated at all values of t* where measurements are made. Consequently, $\mathbf{V}_p$ contains only a single term, which is the variance of the estimated k, σ_k^2. The derivative of Equation 3 with respect to k is

$$\frac{d\,\ln(C_r/C_{tr})}{dk} = \frac{1 - e^{kt_{inj}} + kt_{inj}}{k(e^{kt_{inj}} - 1)} - t^* \tag{5}$$

The variance of the estimated k can now be evaluated using

$$\sigma_k^2 = \sigma^2\left\{\sum_{i=1}^{n}\left[\frac{1 - e^{kt_{inj}} + k\,t_{inj}}{k(e^{kt_{inj}} - 1)} - t^*\right]^2\right\}^{-1} \tag{6}$$

with i = 1 to n, where n is the total number of observations. The 95% confidence interval for k is now given by $k \pm 2\sigma_k$.

Results

Background Concentrations

Large measured concentrations of TOC, TPH-G, and BTEX in ground water suggest that substantial quantities of potential electron donors are present, especially in the heavily contaminated interior of the site (Table 1). The total supply of organic carbon at this site is probably larger than the concentrations in Table 1, because hydrocarbons sorbed to aquifer solids or present as a separate liquid phase are not included in the ground water analyses. It is highly probable that most TOC at the site consists of petroleum hydrocarbons and their breakdown products as concentrations of natural dissolved organic carbon rarely exceed 2 mg/L in pristine environments (Thurman 1985).

Concentrations of TOC, TPH-G, and BTEX were highly spatially variable, as indicated by large coefficients of variation (CV) with regard to the respective mean values (Table 1). Note that nondetects were presumed to have a value of zero for all statistical analyses. The largest concentrations for TOC, TPH-G, and BTEX

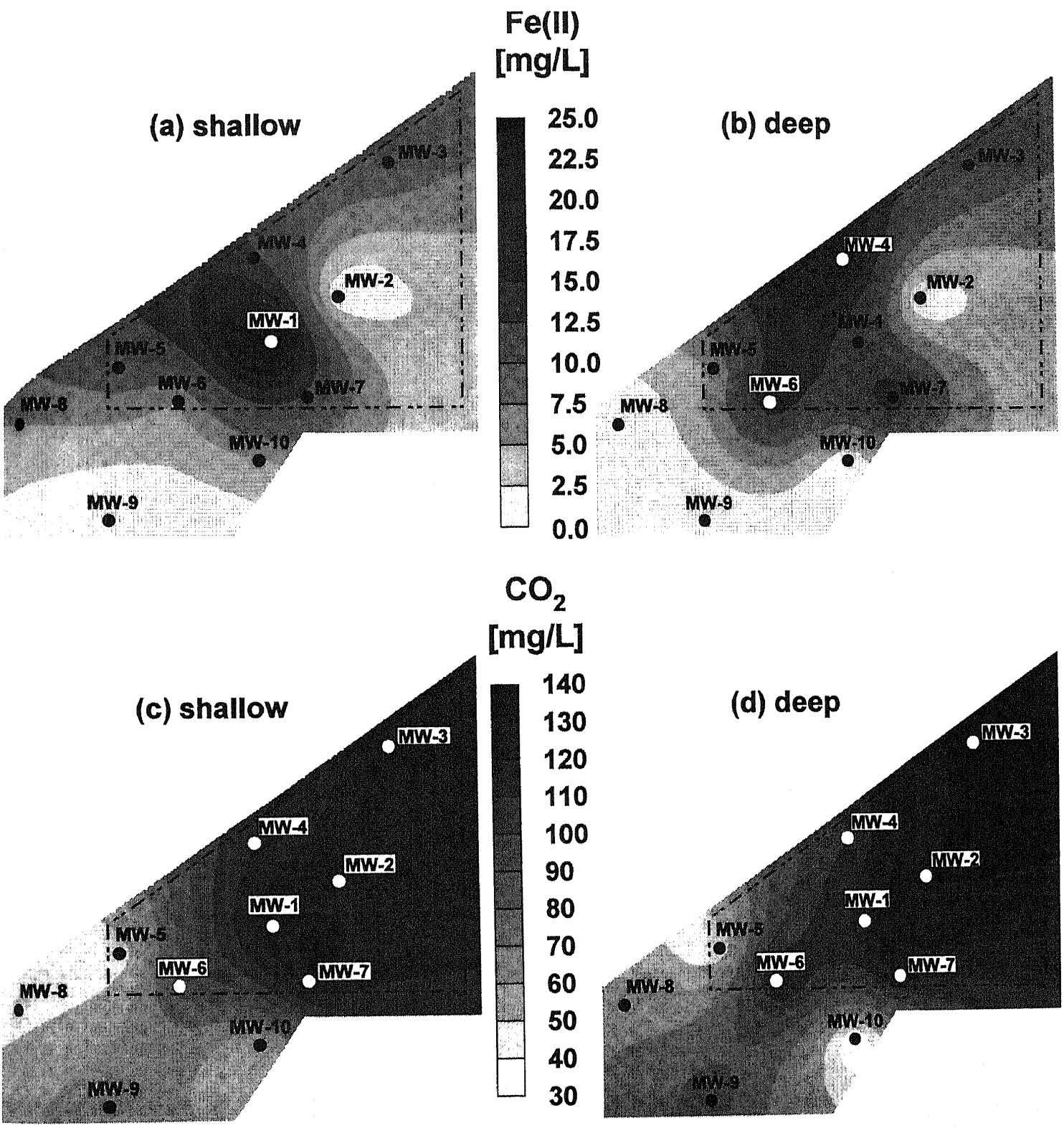

Figure 5. Spatial variability in initial background concentrations of Fe(II) (a and b) and dissolved CO_2 (c and d) in shallow and deep test intervals.

were observed at MW-1, suggesting that most of the fuel was spilled there, while concentrations decreased rapidly with increasing distance from MW-1 (Figure 3a and b). Concentrations of TOC, TPH-G, and BTEX were generally larger in the shallow test interval than in the deep test interval. Concentrations of TPH-G were significantly smaller than those for TOC, suggesting that much of the dissolved organic carbon at the site may consist of higher molecular weight (i.e., > C_{10}) components of diesel fuel. Although concentrations of individual BTEX components are not shown, BTEX consisted primarily of benzene (Figure 3c and d). For example, the BTEX concentration in the shallow test interval at MW-1 was 1725 µg/L and the benzene concentration was 1700 µg/L.

Dissolved O_2 concentrations in ground water entering the site from the north (e.g., at MW-3) were between 2 and 3 mg/L, which is substantially smaller than the air-saturated value (10.2 mg/L) at the site ground water temperature of 15°C. Dissolved O_2 concentrations decreased to ≤ 0.6 mg/L near the center of the site and then increased to 4 mg/L further downgradient (Figure 4). Less variability was observed for SO_4^{2-} concentrations at the site, which generally increased downgradient in both shallow and deep test intervals (Table 1). Concentrations of NO_3^- and NO_2^- were < 0.1 mg/L in both test intervals in all wells.

Concentrations of Fe(II) were largest near MW-1 (shallow test interval) and MW-4 (deep test interval) and decreased with

Table 1
Initial Background Concentrations of Potential Electron Donors, Electron Acceptors, Metabolic Products, and pH, Measured Prior to Conducting Push-Pull Tests

Monitoring Well	Test Interval	TOC (mg/L)	TPH-G (mg/L)	BTEX (µg/L)	O_2 (mg/L)	SO_4^{2-} (mg/L)	Fe(II) (mg/L)	CO_2 (mg/L)	pH
MW-1	shallow	53.3	4.6	1725.2	0.6	7.3	25	130	6.4
	deep	73.0	3.0	903.1	0.5	6.2	10	115	6.4
MW-2	shallow	16.6	1.0	63.8	0.3	8.5	< 5	125	6.4
	deep	17.0	1.0	179.2	2.0	7.1	< 5	130	6.5
MW-3	shallow	14.5	< 0.1	4.5	2.6	7.7	10	125	6.4
	deep	12.0	< 0.1	2.5	2.5	7.4	10	135	6.4
MW-4	shallow	16.2	0.1	8.6	0.5	7.2	13	109	6.4
	deep	11.2	0.3	14.9	0.7	7.5	20	100	6.6
MW-5	shallow	11.4	0.3	36.5	< 0.01	6.8	10	43	6.5
	deep	10.0	0.6	63.9	< 0.01	9.4	5	40	6.5
MW-6	shallow	17.1	< 0.1	23.6	2.8	9.3	5	85	6.6
	deep	17.4	0.3	48.0	1.8	9.1	15	117	6.6
MW-7	shallow	20.7	0.6	152.1	0.05	10.6	12	129	6.4
	deep	2.6	0.6	103.3	0.02	9.3	15	114	6.6
MW-8	shallow	< 0.1	< 0.1	1.3	2.7	8.1	5	47	6.6
	deep	6.3	< 0.1	1.3	2.3	6.2	< 5	65	6.6
MW-9	shallow	1.0	< 0.1	1.9	4.0	8.3	< 5	69	6.7
	deep	< 0.1	< 0.1	4.2	3.6	10.8	< 5	85	6.7
MW-10	shallow	< 0.1	< 0.1	5.0	3.2	14.5	5	48	7.3
	deep	< 0.1	< 0.1	6.5	4.0	17.2	< 5	28	7.4
mean	shallow	15.1	0.67	202.3	1.68	8.83	8.5	91.0	6.57
CV(%)	shallow	103	214	266	91	26	88	41	4
mean	deep	15.0	0.58	132.7	1.74	9.03	7.5	92.9	6.63
CV(%)	deep	143	156	209	82	36	101	40	4

increasing distance from these wells (Figure 5a and b). Dissolved CO_2 concentrations were largest near the interior of the site and generally decreased downgradient (Figure 5c and d). Values of pH showed little variation across the site (Table 1).

Aerobic Respiration Tests

During aerobic respiration, O_2 is reduced to water during the concurrent oxidation of organic carbon to CO_2:

$$[CH_2O] + O_2 \rightarrow CO_2 + H_2O \qquad (7)$$

where $[CH_2O]$ is a generic formula for a source of organic carbon (note that this reaction is used for illustration only). Thus indirect evidence for aerobic respiration at the site is given by reduced dissolved O_2 concentrations and elevated dissolved CO_2 concentrations in some locations (e.g., in the shallow test intervals in MW-2 and MW-5 and in the deep test intervals at MW-5 and MW 7; Table 1). However, aerobic respiration may also be occurring in locations where dissolved O_2 and organic carbon concentrations are both elevated (e.g., near MW-4).

The extracted Br^- mass for all aerobic respiration tests ranged from 27 to 100% of the injected Br^- mass, with a mean of 77% and a CV of 25%. The extracted dissolved O_2 mass ranged from 20 to 66% of the injected dissolved O_2 mass, with a mean of 42% and a CV of 31%. The residence time for the test solutions in the aquifer ranged from 64 to 140 minutes, with a mean of 96 minutes and a CV of 23 minutes. In this context, the residence time is defined as the time interval from the instant when 50% of the test solution is injected into the aquifer to the instant when 50% of the injected Br^- mass is extracted. It was assumed that the transport properties of Br^- and dissolved O_2 are identical in the aquifer so that the mass of O_2 consumed is proportional to the area between the Br^- and dissolved O_2 breakthrough curves (note that this assumption was demonstrated to be valid in similar push-pull tests performed by Istok et al. [1997]). Thus, if no O_2 consumption occurred during the test, the two curves would be identical. However, dissolved O_2 breakthrough curves had generally lower peak concentrations and substantially smaller areas than Br^- breakthrough curves. This is illustrated by the breakthrough curve for the test in the deep interval of MW-2 (Figure 6a). In Figure 6a, measured Br^- and dissolved O_2 concentrations are plotted as "relative concentrations," C/C^o, where C is the measured concentration of either solute and C^o is the known concentration of the same solute in the injected test solution. The x-axis shows time as elapsed time since the end of the test solution injection, t* (see Equation 2). In this test, only 39% of the injected dissolved O_2 mass was extracted (Figure 6a), compared to 87% of the injected Br^- mass, indicating substantial O_2 consumption (~ 55%) during the test. Here, O_2 or NO_3^- consumption is calculated as [1 − (extracted O_2 or NO_3^- mass fraction / extracted Br^- mass fraction)] × 100%. Dissolved O_2 consumption displayed substantial spatial variability with values ranging from ~ 0% in the deep test interval in MW-8 to ~ 73% in the shallow test interval in MW-4 (data not shown).

First-order rate coefficients for aerobic respiration were computed by fitting Equation 3 to experimental breakthrough data (Table 2). For example, for the test in the deep interval of MW-2, k was 0.65 h^{-1} and $2\sigma_k$ was 0.09 h^{-1} (Figure 6b). Note that the best fit line in Figure 6b is intentionally extended to the y-axis intercept,

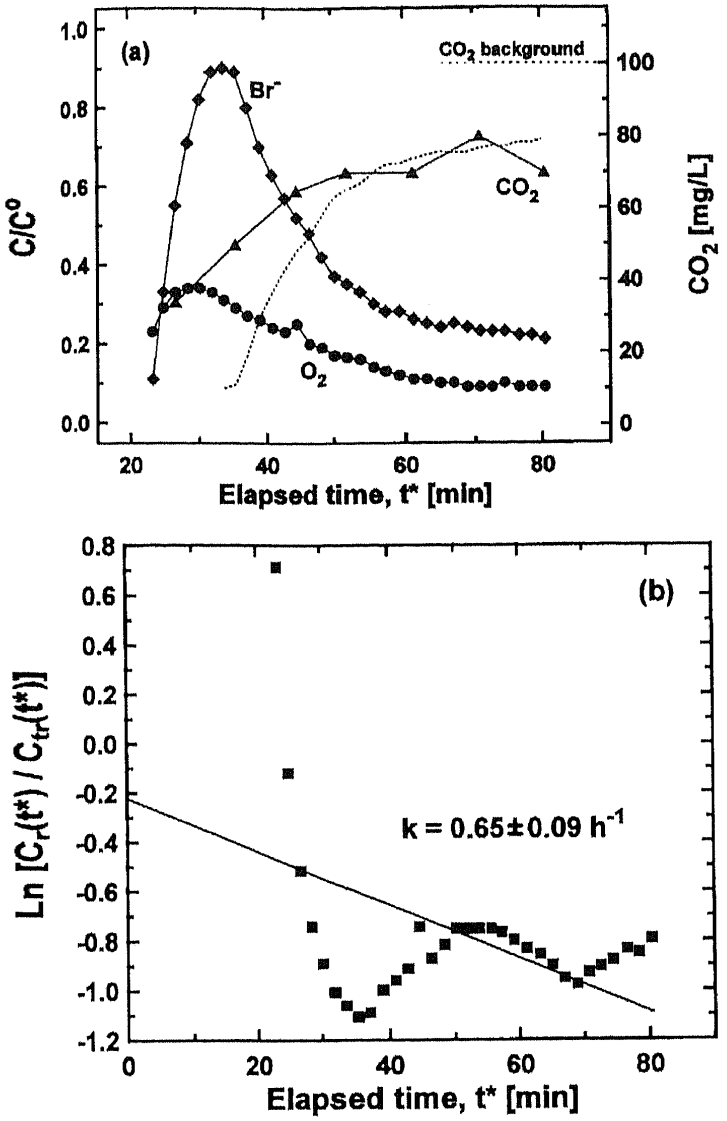

Figure 6. (a) Example breakthrough curves for aerobic respiration test performed in the deep interval of MW-2 (t_{inj} = 42.6 minutes). The dashed line represents computed CO_2 concentrations based on the dilution of site ground water by the injection solution. (b) Associated regression plot for rate coefficient determination, obtained by fitting Equation 3 to the experimental data using a nonlinear least-squares routine.

Table 2
Computed Aerobic Respiration and Denitrification Rate Coefficients, k with 95% Confidence Intervals ($k \pm 2\sigma_k$) Using the Method of Haggerty et al. (1998)

		Aerobic Respiration		Denitrification	
Monitoring Well	Test Interval	k [h^{-1}]	$2\sigma_k$ [h^{-1}]	k [h^{-1}]	$2\sigma_k$ [h^{-1}]
MW-1	shallow	0.22	0.06	0.22	0.03
	deep	0.31	0.07	0.21	0.03
MW-2	shallow	0.33	0.11	0.30	0.04
	deep	0.65	0.09	0.21	0.04
MW-3	shallow	0.42	0.04	0.23	0.04
	deep	0.41	0.04	0.24	0.04
MW-4	shallow	1.69	0.14	0.25	0.03
	deep	0.75	0.07	0.27	0.04
MW-5	shallow	0.37	0.07	0.14	0.03
	deep	0.83	0.16	0.21	0.03
MW-6	shallow	0.49	0.07	0.15	0.03
	deep	0.55	0.06	0.26	0.06
MW-7	shallow	0.82	0.06	0.42	0.06
	deep	0.63	0.04	0.16	0.03
MW-8	shallow	0.15	0.05	0.17	0.03
	deep	0.08	0.02	0.11	0.02
MW-9	shallow	0.24	0.02	0.09	0.02
	deep	0.52	0.05	0.28	0.03
MW-10	shallow	0.35	0.04	0.31	0.03
	deep	0.44	0.03	0.27	0.03
mean	shallow	0.51	0.07	0.23	0.03
CV(%)	shallow	90	53	43	32
mean	deep	0.52	0.06	0.22	0.04
CV(%)	deep	43	64	24	31

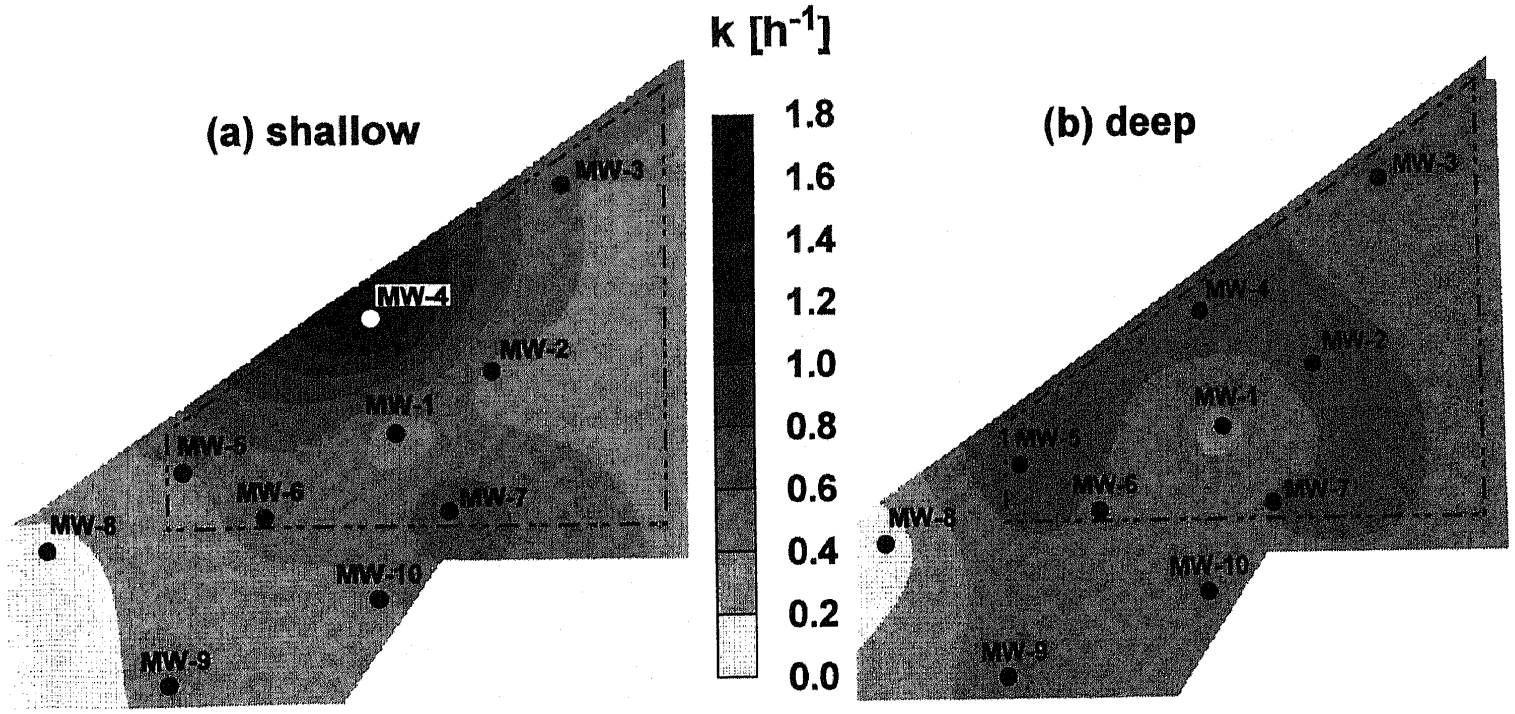

Figure 7. Spatial variability in first-order reaction rate coefficients for aerobic respiration in (a) shallow and (b) deep test intervals.

since both slope and y-axis intercept were fitted in this approach (Equation 3). While temporal trends are visible in the experimental data (Figure 6b), fitting both slope and intercept improves the robustness of this method (Haggerty et al. 1998), leading to $2\sigma_k$ values that in most cases are < 20% of the estimated values of k (Table 2). Alternate kinetic models (zero- and nth order) were fit to the experimental data by Conner (1997). However, employing these models did not significantly reduce the magnitude of the respective $2\sigma_k$ values. Aerobic respiration rates in the shallow test interval were highly spatially variable; the largest rates were obtained for tests conducted in MW-4 and rates decreased sharply in tests conducted further downgradient (Figure 7a). Aerobic respiration rates were much less spatially variable in the deep test interval (Figure 7b).

Dissolved CO_2 concentrations increased during the extraction phase of aerobic respiration tests (Figure 6a), which may be attributed in part to microbial CO_2 production (Equation 7). However, the interpretation of dissolved CO_2 concentrations during extraction phase pumping is complicated by the presence of large background dissolved CO_2 concentrations in site ground water (Table 1). This creates the possibility that increasing dissolved CO_2 concentrations during extraction phase pumping are not due to microbial CO_2 production but are simply due to the decreasing dilution of site ground water by the injected test and clean water flushing solutions (which contained no dissolved CO_2). For example, in Figure 6a, dissolved CO_2 concentrations increased during extraction phase pumping and approached the CO_2 background concentration of 100 mg/L, as measured at the conclusion of the pre-test purging for this test. Note that this background concentration differs from the initial background data presented in Table 1, due to temporal variability in subsurface conditions caused primarily by recharge. Using the Br^- breakthrough curve as a measure of the degree of dilution of site ground water by injected solutions, CO_2 concentrations were computed based on dilution of site ground water alone (dashed line, Figure 6a). Measured CO_2 concentrations were significantly higher than computed CO_2 concentrations during a large portion of the extraction phase, supporting the conclusion that substantial CO_2 production occurred during this test. Similar results were obtained for the other aerobic respiration tests (data not shown).

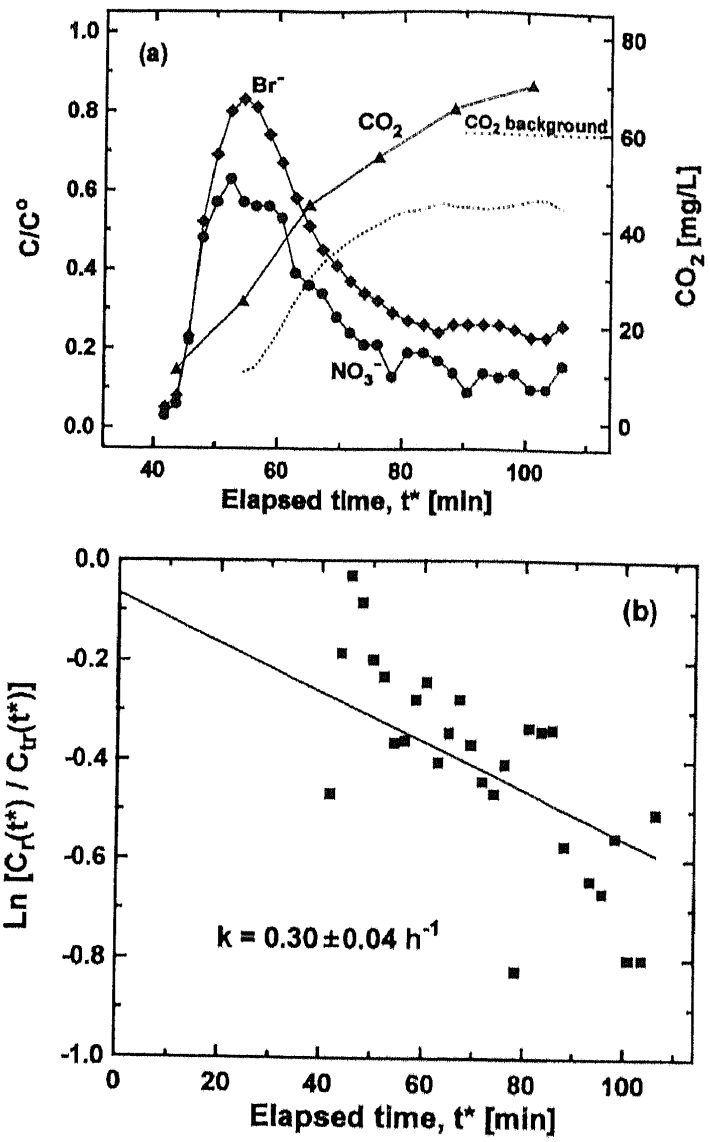

Figure 8. (a) Example breakthrough curves for denitrification test performed in the shallow interval of MW-2 (t_{inj} = 26.7 minutes). The dashed line represents computed CO_2 concentrations based on the dilution of site ground water by the injection solution. (b) Associated regression plot for rate coefficient determination, obtained by fitting Equation 3 to the experimental data using a nonlinear least-squares routine.

Denitrification Tests

During denitrification, NO_3^- is reduced to N_2 gas in a series of steps with the oxidation of organic carbon to CO_2:

$$[CH_2O] + NO_3^- \rightarrow NO_2^- + CO_2 + H_2O \quad (8a)$$

$$[CH_2O] + NO_2^- \rightarrow NO + CO_2 + H_2O \quad (8b)$$

$$[CH_2O] + NO \rightarrow N_2O + CO_2 + H_2O \quad (8c)$$

$$[CH_2O] + N_2O \rightarrow N_2 + CO_2 + H_2O \quad (8d)$$

where again $[CH_2O]$ represents a generic carbon source. Thus, indirect evidence for denitrification would be given by reduced NO_3^- concentrations, elevated NO_2^-, NO, N_2O, or N_2 concentrations, and elevated dissolved CO_2 concentrations. However, at this site NO_3^- and NO_2^- background concentrations were uniformly below detection (< 0.1 mg/L) and provide no useful information on locations where denitrifying activity may be occurring.

The extracted Br^- mass for all denitrification tests ranged from 68 to 100% of the injected Br^- mass, with a mean of 86% and a CV of 13%. The extracted NO_3^- mass ranged from 51 to 81% of the injected NO_3^- mass, with a mean of 64% and a CV of 14%. The residence time for the test solutions in the aquifer ranged from 77 to 143 minutes, with a mean of 97 minutes and a CV of 18 minutes. It was assumed that the transport properties of Br^- and NO_3^- were identical so that the magnitude of NO_3^- consumed is proportional to the area between the Br^- and NO_3^- breakthrough curves. In general, NO_3^- breakthrough curves had lower peak concentrations and substantially smaller areas than Br^- breakthrough curves. This is illustrated by the breakthrough curve for the test in the shallow interval of MW-2 (Figure 8a). In this test, only 52% of the injected NO_3^- mass was extracted, compared to 83% for Br^-, indicating substantial NO_3^- consumption (~ 37%) during the test. Nitrate consumption displayed substantial spatial variability with values ranging from ~ 3% in the shallow test interval in MW-5 to ~ 36% in the shallow test interval in MW-7 (data not shown). Increasing concentrations of dissolved CO_2 were measured during the extraction phase of denitrification tests (Figure 8a; CO_2 background concen-

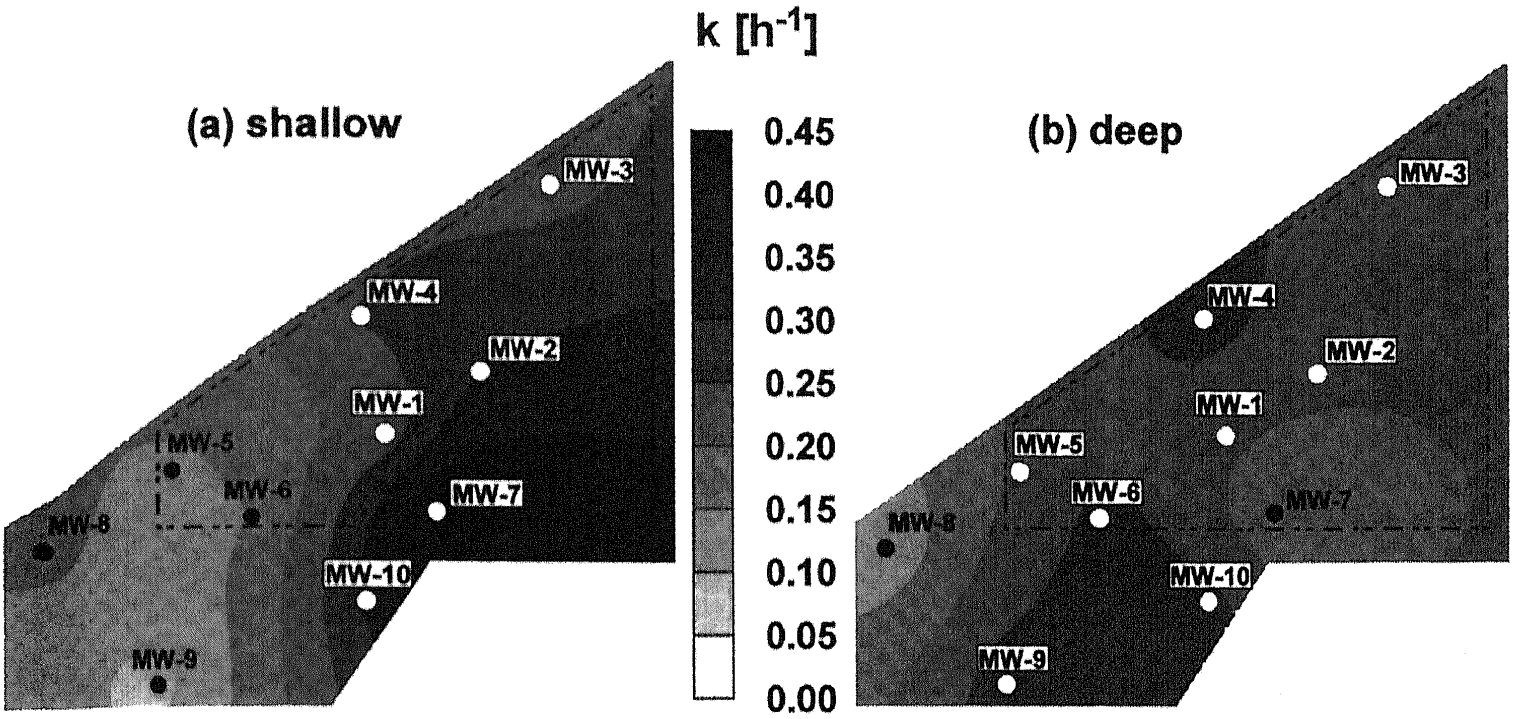

Figure 9. Spatial variability in first-order reaction rate coefficients for denitrification in (a) shallow and (b) deep test intervals.

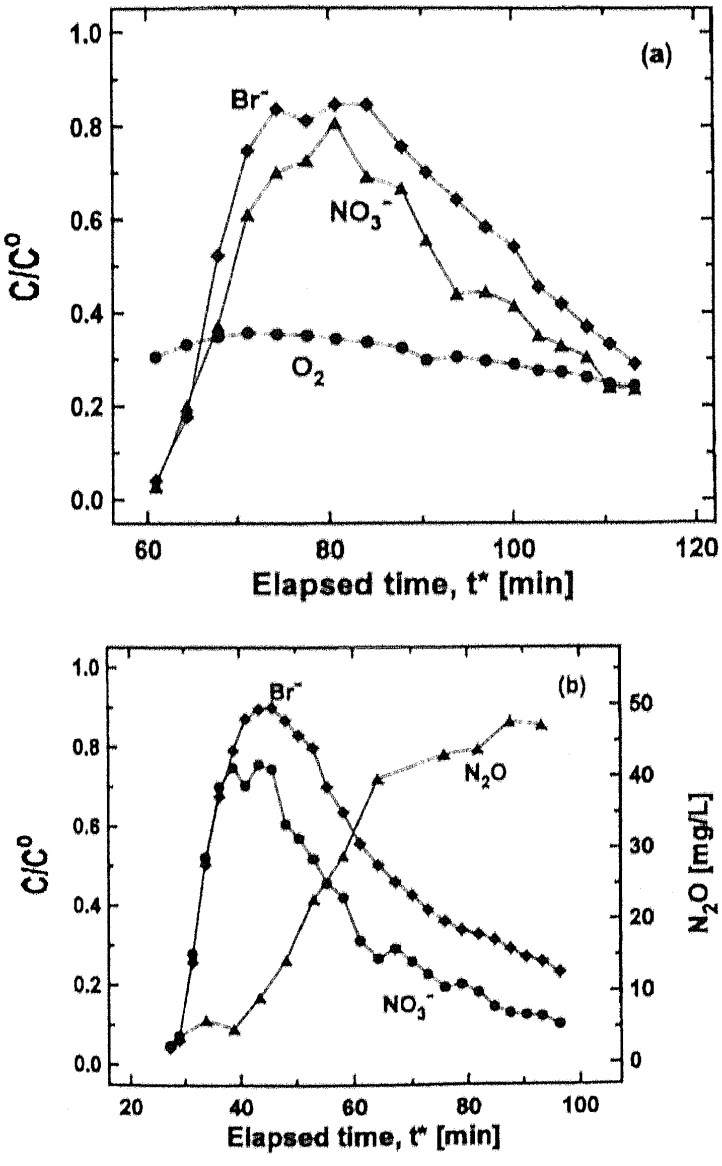

Figure 10. Breakthrough curves for additional denitrification tests in MW-3 with (a) dissolved O_2 and (b) dissolved C_2H_2 in test solution.

tration was 60 mg/L, measured at the conclusion of the pre-test purging), which is attributed in part to microbial production of CO_2 (Equation 8), as discussed in the previous section.

First-order rate coefficients for denitrification were computed by fitting Equation 3 to experimental breakthrough data (Table 2). For example, for the test in the shallow interval of MW-2, k was 0.30 h^{-1}, and $2\sigma_k$ was 0.04 h^{-1} (Figure 8b). Denitrification rates were highly spatially variable; the largest rates were computed for tests conducted in MW-7 (Figure 9).

Verification of Microbial Metabolic Activity

Substantial consumption of injected dissolved O_2 was observed in the aerobic respiration test conducted in the deep test interval of MW-3 prior to the treatment of this portion of the aquifer with sodium hypochlorite, and the computed rate coefficient was 0.41 h^{-1} with $2\sigma_k$ of 0.04 h^{-1} (Table 2). When the aerobic respiration test was repeated at the same location after the sodium hypochlorite treatment, the extracted O_2 mass was almost identical to the extracted Br^- mass, and the computed rate coefficient decreased to essentially zero. However, breakthrough curves for Br^- were radically different in tests conducted before and after sodium hypochlorite treatment (data not shown), which suggests that the sodium hypochlorite may have caused additional changes in aquifer properties.

Substantial consumption of injected NO_3^- (~ 19%) was observed in the denitrification test conducted in the deep test interval of MW-3, and the computed rate coefficient was 0.24 h^{-1} with $2\sigma_k$ of 0.04 h^{-1} (Table 2). However, when dissolved O_2 was included in the injected test solution to inhibit anaerobic denitrifying activity, NO_3^- consumption decreased to ~ 11% and the computed rate coefficient for denitrification decreased to 0.12 h^{-1} with $2\sigma_k$ of 0.02 h^{-1} (Figure 10a). The rate coefficient for aerobic respiration in this test was 0.32 h^{-1} with $2\sigma_k$ of 0.08 h^{-1}.

Additional tests were conducted using test solutions containing dissolved C_2H_2. The presence of C_2H_2 inhibits nitrous oxide reductase, the terminal enzyme of the denitrification pathway, thus blocking the conversion of N_2O to N_2 (Equation 8d), and increasing concentrations of dissolved N_2O were observed during the

extraction phase in these tests. This is illustrated for the test in the deep interval of MW-3 (Figure 10b). The denitrification rate coefficient in this test was 0.28 h^{-1} with $2\sigma_k$ of 0.05 h^{-1}. Dissolved C_2H_2 was apparently transported conservatively during these tests as its breakthrough curves were virtually identical to the breakthrough curves for Br^- (data not shown).

Discussion

In a previous study, we demonstrated that the push-pull test method is useful for quantifying a variety of subsurface microbial activities in situ (Istok et al. 1997). In this study we have demonstrated that the push-pull test can also be used to quantify site-scale spatial variability in microbial activities. This is illustrated by reasonably small 95% confidence intervals for estimated rate coefficients across a petroleum-contaminated site (Table 2). Both studies indicated good reproducibility of test results. In this study, rate coefficients of aerobic respiration and denitrification determined from additional push-pull tests in selected locations (aimed at verifying microbially mediated electron acceptor consumption; see previous section) agreed well with rate coefficients determined from previous push-pull tests at the same locations (Table 2).

In general, rates of microbial activities reported here are considerably higher than those reported in other recent studies. For example, previous estimates of first-order aerobic respiration rate coefficients in petroleum-contaminated aquifers have ranged from 0.4×10^{-3} h^{-1} (Chiang et al. 1989) to 0.02 h^{-1} (Nielsen et al. 1996), whereas estimates at this site ranged from 0.08 to 1.69 h^{-1} (Table 2). Similarly, the denitrification rate coefficients we determined were up to two orders of magnitude larger than several recently determined rate coefficients of denitrification (e.g., Starr and Gillham 1989; Reinhard et al. 1997). Obviously, many factors such as the specific types and concentrations of electron donors could contribute to these differences. However, it is important to note that our approach assumed that the microbial processes we investigated are electron acceptor limited, and that the high concentrations of electron acceptors in the injected test solutions will support maximal rates of electron donor oxidation, and not the intrinsic rate of activity which is supported by ambient concentrations of electron acceptors in site ground water.

Furthermore, our rate estimates were based on measurements of electron acceptor consumption and may have included contributions from abiological reactions such as the oxidation of Fe(II) by O_2 or by NO_3^- (chemodenitrification). However, the relatively small aerobic respiration rate coefficients determined in both intervals of MW-1 (Table 2), despite the presence of high concentrations of Fe(II) (Table 1), provide some evidence that abiological reactions such as O_2-dependent Fe(II) oxidation are not major contributors to the observed rates of electron acceptor consumption at this site. To corroborate this argument, we computed the theoretical maximum contribution of dissolved Fe(II) to the O_2 consumption for selected tests, accounting for the dilution of our test solutions by site ground water using Br^- breakthrough data and Fe(II) background concentrations from Table 1 (see previous calculations for CO_2 production). For example, for the test in the shallow interval of MW-1, 382 mg Fe(II) should have come in contact with our test solution, which could account for 16.8% of the O_2 consumed during this test. For the test in the shallow interval of MW-4 (highest aerobic respiration rate coefficient at this site; Table 2), 287 mg Fe(II) should have come in contact with our test solution, which could account for 5.5% of the observed O_2 consumption during this test. However, while these calculations confirm the limited significance of dissolved Fe(II) contribution to the overall O_2 consumption, we cannot eliminate the possibility that solid-phase Fe(II) could also have interacted with our test solutions, i.e., $FeCO_3(s)$ (e.g., Stumm and Morgan 1981), and its contribution to observed O_2 consumption at the site remains uncertain.

Conversely, it is interesting to note that the highest rates of both aerobic respiration and denitrification found in other recent studies have been determined using in situ microcosm (ISM) studies rather than the more conventional natural gradient tracer tests (Bjerg et al. 1996; Gillham et al. 1990). Furthermore, it is interesting to note that the more widely accepted geochemical methods of determining subsurface microbial activities provide activity estimates which underestimate rates derived using radioisotope data by factors ranging from 10^4 to 10^6 (Phelps et al. 1994). Together, these results provide some additional credibility to the high aerobic respiration and denitrification rates that were determined in situ in this study.

We used several approaches to discriminate the role of biological agents in the observed electron acceptor-consuming activities. The first and simplest of these approaches was to examine whether the production of CO_2 occurred concurrently with electron acceptor consumption. In a biologically catalyzed process, CO_2 production and electron acceptor consumption should be temporally related because the catabolism of organic electron donors to CO_2 requires the concurrent use of electron acceptors to allow the regeneration of oxidized cofactors such as nicotine adenine dinucleotide (NAD^+). No production of CO_2 should occur in an abiological process such as Fe(II) oxidation by O_2:

$$Fe(II) + 1/4O_2 + 2OH^- + 1/2H_2O \rightarrow Fe(OH)_3 \qquad (9)$$

It has been demonstrated previously that the stoichiometry of HCO_3^-/CO_2 production and electron acceptor consumption during push-pull-type tests is close to predicted values for both aerobic respiration (Istok et al. 1997) and denitrification using model electron donors such as glucose (Trudell et al. 1986). These calculations were not performed in this study, because the stoichiometries of O_2 or NO_3^- consumption and CO_2 production are substrate-specific. It is therefore inappropriate to use these ratios to estimate rates of catabolism of mixtures of electron donors (Hickey 1995). In addition, no routine measurements for total carbonate and pH were conducted during the extraction phase of the push-pull tests, impeding a fully quantitative interpretation of the available CO_2 data. However, the push-pull test breakthrough curves for aerobic respiration and denitrification obtained at this site (Figures 6a and 8a) demonstrated concurrent CO_2 production and electron acceptor consumption, and therefore qualitatively suggest that the observed electron acceptor consumption involved a substantial biological component.

Our second approach involved the use of a variety of inhibitors to investigate the role of microorganisms in electron acceptor consumption. Unfortunately, in the case of aerobic respiration, the range of inhibitors available for this study was limited. Simple and effective inhibitors of aerobic respiration such as cyanide (CN^-) or azide (N_3^-) could not be used because of their considerable human toxicity and the potential for off-site transport of these compounds in ground water. Using a sodium hypochlorite treatment, we demonstrated an inhibition of O_2 consumption. However, sodium hypochlorite may also have removed much of the abiotic O_2 demand due to its strong oxidizing capability, e.g., by oxidizing dissolved Fe(II) or even $FeCO_3(s)$. In addition, other physical and chemical parameters (e.g., pH) were likely altered during this test. Together, these unde-

sired effects rendered the results of the sodium hypochlorite treatment test inconclusive, and we therefore cannot unequivocally estimate the contribution of abiotic reactions to the observed rates of O_2 consumption.

More subtle inhibitors of denitrifying activity were available for our experiments. For example, denitrification is inhibited by the presence of O_2 through complex effects on both the activity and synthesis of key enzymes in the denitrification pathway (Tiedje 1988). Consistent with these effects we observed that the presence of O_2 reduced the rate of NO_3^- consumption by approximately 50% (Figure 10a). This incomplete inhibition of NO_3^- consumption could reflect the contribution of abiotic reactions and this would lead to more conservative, although still substantial, estimates of denitrification rates at this site. However, it is important to note that significant O_2 consumption also occurred during this experiment (Figure 10a). Because NO_3^- reduction is the least O_2-sensitive of the enzyme activities associated with denitrification (Hernandez and Rowe 1987), we cannot eliminate the possibility that the depletion of O_2 allowed concurrent NO_3^- consumption to occur in parts of the push-pull test environment.

The most unequivocal inhibitor used was C_2H_2. The inhibition of N_2O reductase activity by C_2H_2 is the basis of the "acetylene-blockage" assay which has been successfully used to estimate denitrifying activity in a wide variety of environments (Keeney 1986). Our results demonstrated that the presence of C_2H_2 led to the accumulation of N_2O (Figure 10b). This strongly supports the conclusion that observed NO_3^- consumption at this site is biologically mediated. Conversely, the accumulation of N_2O also indicates that the NO_3^- consumption was not due to the activities of microorganisms which catalyze dissimilatory nitrate reduction to ammonia (DNRA) under anaerobic conditions. Although DNRA is sensitive to O_2 and often occurs in environments with high C/N ratios similar to those found at the present site, this process is insensitive to C_2H_2 and does not involve N_2O as an intermediate (Tiedje 1988). A further interesting aspect of our results with C_2H_2 is that recovery of N_2O was delayed with respect to the Br^- tracer (Figure 10b). A similar effect was observed by Smith et al. (1996), who attributed their observation to a "lag phase" in N_2O production that is known to occur during the acetylene blockage assay.

Despite some unresolved questions concerning the relative contributions of biological and abiological processes in electron acceptor consumption, our results clearly indicate that there is considerable spatial variation in potential microbial activities throughout the site (Figures 7 and 9). Although the patterns are complex, some general trends can be observed. For example, the highest rates of O_2 consumption were found in the shallow upgradient portions of the site near MW-4 (Figure 7a). This result is not unexpected, as this is the location where uncontaminated oxygenated ground water would be expected to first contact the petroleum-contaminated portion of the aquifer. Further downgradient, the level of petroleum contamination was found to be centered predominantly around MW-1 (Figure 3a and b). The ground water in this environment was found to be anoxic and contained high concentrations of Fe(II) (Figure 5a and b). These geochemical features suggest that the microbial activity at this location was dominated by anaerobic processes. This conclusion is supported by the relatively low rates of aerobic respiration measured at both depth intervals at MW-1 (Table 2).

Beyond these general observations, we were unable to detect any significant correlations between the distribution of the potential microbial activities and likely important variables such as electron donor or acceptor concentrations. While these correlations might be more apparent if the limited abiological component to the electron acceptor usage rates could be removed with confidence, the lack of significant correlations may be regarded as indicative of the complex nature of microbial metabolic activities in contaminated subsurface environments. For example, denitrifying activity is known to be strongly influenced by a number of factors including the availability of nitrate, the availability of an electron donor (C-source), temperature, O_2 concentration, and pH, although good correlations between activity and any individual parameter are rarely observed (Korom 1992). Previous laboratory studies of denitrification using subsurface materials have consistently demonstrated that this activity shows considerable spatial variability (e.g., Christensen et al. 1990; Parkin 1987) and is often log-normally distributed in soil samples. This skewed distribution is consistent with the existence of localized "hot spots" of activity which are established when one variable (e.g., C-availability) predominates over the numerous other variables known to affect the environmental distribution and activity of soil microorganisms. Log-normal distributions of microbial activity have also been reported in studies of methanogenesis (Adrian et al. 1994) and aerobic respiration (Parkin and Robinson 1992).

Conclusions

The single-well, push-pull test method was used to quantify the spatial variability in rates of selected microbial metabolic activities in situ in the saturated zone of a petroleum-contaminated, unconfined alluvial aquifer. The push-pull test method was successful in measuring rates of consumption of injected electron acceptors (O_2 for aerobic respiration tests and NO_3^- for denitrification tests) in the presence of abundant petroleum hydrocarbons and their breakdown products to serve as electron donors. Significant horizontal and vertical variability in aerobic respiration and denitrification rates was observed. The highest rates of aerobic respiration occurred near the upgradient edge of the contamination zone, where the microbial population was apparently best adapted to conditions of high carbon concentrations and continuous inputs of dissolved O_2 from upgradient. The highest rates of denitrification were observed downgradient from locations of the highest rates of aerobic respiration, where dissolved O_2 concentrations were low but carbon levels were still high.

We provided strong qualitative evidence that observed electron acceptor consumption at this site was largely biologically mediated. However, we were unable to quantitatively delineate the contribution of biological and abiological processes to the electron acceptor consumption. Nonetheless, while some of our results, such as the effect of O_2 on NO_3^- consumption (Figure 10a), might decrease our rate estimates by a factor of two, this is clearly insufficient to account for differences between rates obtained in this study and rates obtained by others which are often separated by more than one order of magnitude. In this respect, it is important to note that the rates we determined represent maximal rates of aerobic respiration and denitrification due to the high concentrations of electron acceptors in the injected test solutions, and not intrinsic rates which are supported by ambient concentrations of electron acceptors in site ground water. On the other hand, it is noteworthy that the rates we determined show closest agreement with rates found in other in situ studies and that there is evidence that rates may be significantly

underestimated using non-in situ techniques. Together, these findings suggest that results obtained using in situ test methods, such as the push-pull test, may provide more accurate rate estimates of subsurface microbial metabolic activities. Further studies will be required to compare the results of these types of techniques in similar environments.

Acknowledgments

Financial support for this project was provided by Chevron Research and Technology Co., Richmond, California, and the National Center for Integrated Bioremediation Research and Development, Ann Arbor, Michigan. Additional financial support was provided by the Office of Research and Development, U.S. Environmental Protection Agency, under agreement R-815738-01 through the Western Region Hazardous Substance Research Center. The content of this paper does not necessarily represent the views of the agency. The authors would like to thank M. Humphrey and J. Guida for their help in the field and laboratory. Helpful review comments by Dr. R. Allen-King were greatly appreciated.

References

Adrian, N.R., J.A. Robinson, and J.M. Suflita. 1994. Spatial variability in biodegradation rates as evidenced by methane production from an aquifer. *Applied and Environmental Microbiology* 60, no. 10: 3632-3639.

American Public Health Association (APHA), American Water Works Association, and Water Environment Federation. 1992. Standard methods for the examination of water and wastewater (18th ed.), ed. A.E. Greenberg, L.S. Clesceri, and A.D. Eaton. Washington, D.C.: APHA.

Balderston, W.L., B. Sherr, and W.J. Payne. 1976. Blockage by acetylene of nitrous oxide reduction in Pseudomonas perfectomarinus. *Applied and Environmental Microbiology* 31, no. 4: 504-508.

Balkwill, D.L., F.R. Leach, J.T. Wilson, J.F. McNabb, and D.C. White. 1988. Equivalence of microbial biomass measures based on membrane lip and cell wall components, adenosine triphosphate, and direct counts in subsurface aquifer sediments. *Microbial Ecology* 16, no. 1: 73-84.

Bard, Y. 1974. *Nonlinear Parameter Estimation.* New York: Academic Press.

Bjerg, P.L., A. Brun, P.H. Nielsen, and T.H. Christensen. 1996. Application of a model accounting for kinetic sorption and degradation to in situ microcosm observations on the fate of aromatic hydrocarbons in an aerobic aquifer. *Water Resources Research* 32, no. 6: 1831-1841.

Bowman, J.P., L. Jimenez, I. Rosario, T.C. Hazen, and G.S. Sayler. 1993. Characterization of the methanotrophic bacterial community present in a trichloroethylene-contaminated subsurface groundwater site. *Applied and Environmental Microbiology* 59, no. 8: 2380-2387.

Brock, T.D., and M.T. Madigan. 1991. *Biology of Microorganisms*, 6th ed. Englewood Cliffs, New Jersey: Prentice Hall.

Chiang, C.Y., J.P. Salanitro, I.Y. Chai, J.D. Colthart, and C.L. Klein. 1989. Aerobic biodegradation of benzene, toluene, and xylene in a sandy aquifer – data analysis and computer modeling. *Ground Water* 27, no. 6: 823-834.

Christensen, S., S. Simkins, and J.M. Tiedje. 1990. Spatial variation in denitrification: Dependency of activity centers on the soil environment. *Soil Science Society of America Journal* 54, no. 6: 1608-1613.

Conner, G.T. 1997. Spatial variability in aerobic respiration and denitrification in a petroleum contaminated groundwater aquifer. M.S. thesis engineering report, Department of Civil, Construction, and Environmental Engineering, Oregon State University, Corvallis, Oregon.

Cozzarelli, I.M., R.P. Eganhouse, and M.J. Baedecker. 1988. The fate and effects of crude oil in a shallow aquifer: II Evidence of anaerobic degradation of monoaromatic hydrocarbons. In U.S. Geological Survey (USGS) Toxic Substances Hydrology Program, Proceedings of the Technical Meeting, Phoenix, Arizona, September 26-30, ed. G.E. Mallard and S.E. Ragone, 21-33. USGS Water-Resources Investigations Report 88-4220.

Draper, N.R., and H. Smith. 1981. *Applied Regression Analysis*, 2nd ed. New York: John Wiley.

Federle, T.W., R.M. Ventullo, and D.C. White. 1990. Spatial distribution of microbial biomass, activity, community structure, and the biodegradation of linear alkylbenzene sulfonate (LAS) and linear alcohol ethoxylate (LAE) in the subsurface. *Microbial Ecology* 20, no. 3: 297-313.

Ghiorse, W.C., and J.L. Wilson. 1988. Microbial ecology of the terrestrial subsurface. *Advances in Applied Microbiology* 33, 107-172.

Gillham, R.W., R.C. Starr, and D.J. Miller. 1990. A device for in situ determination of geochemical transport parameters. 2. Biochemical reactions. *Ground Water* 28, no. 6: 858-862.

Haggerty, R., M.H. Schroth, and J.D. Istok. 1998. Simplified method of "push-pull" test data analysis for determining in situ reaction rate coefficients. *Ground Water* 36, no. 2: 314-324.

Harvey, R.W., R.L. Smith, and L. George. 1984. Effect of organic contamination upon microbial distributions and heterotrophic uptake in a Cape Cod, Mass., aquifer. *Applied and Environmental Microbiology* 48, no. 6: 1197-1202.

Hernandez, D., and J.J. Rowe. 1987. Oxygen regulation of nitrate uptake in denitrifying Pseudomonas aeruginosa. *Applied and Environmental Microbiology* 53, no. 4: 745-750.

Hickey, W.J. 1995. In situ respirometry: Field methods and implications for hydrocarbon biodegradation in subsurface soils. *Journal of Environmental Quality* 24, no. 4: 583-588.

Istok, J.D., M.D. Humphrey, M.H. Schroth, M.R. Hyman, and K.T. O'Reilly. 1997. Single-well, "push-pull" test for in situ determination of microbial metabolic activities. *Ground Water* 35, no. 4: 619-631.

Jorgensen, B.B. 1989. Biogeochemistry of chemoautotrophic bacteria. In *Autrotrophic Bacteria,* ed. H.G. Schlegel and B. Bowien, 117-146. Madison, Wisconsin: Science Tech.

Keeney, D.R. 1986. Critique of the acetylene blockage technique for field measurement of denitrification. In Field measurement of dintrogen fixation and denitrification, ed. R. D. Hauck, and R.W. Weaver, 103-115. Special Publication # 18. Madison, Wisconsin: Soil Science Society of America.

Kelly, F.X., K.J. Dapsis, and D.A. Lauffenburger. 1988. Effect of bacterial chemotaxis on dynamics of microbial competition. *Microbial Ecology* 16, no. 2: 115-131.

Korom, S.F. 1992. Natural denitrification in the saturated zone: A review. *Water Resources Research* 28, no. 6: 1657-1668.

Lovley, D.R., and S. Goodwin. 1988. Hydrogen concentrations as an indicator of the predominant terminal electron-accepting reactions in aquatic sediments. *Geochemica et Cosmochimica Acta* 52, no. 12: 2993-3003.

Madsen, E.L. 1991. Determining in situ biodegradation: Facts and challenges. *Environmental Science and Technology* 25, no. 10: 1663-1673.

McAllister, P.M., and C.Y. Chiang. 1994. A practical approach to evaluating natural attenuation of contaminants in groundwater. *Ground Water Monitoring and Remediation* 14, no. 2: 161-173.

Nielsen, P.H., T.H. Christensen, H.-J. Albrechtsen, and R.W. Gillham. 1996. Performance of the in situ microcosm technique for measuring the degredation of organic chemicals in aquifers. *Ground Water Monitoring and Remediation* 16, no. 1: 130-140.

Oregon Department of Environmental Quality (ODEQ). 1990. ODEQ laboratory method OR-TPH-G (Total Petroleum Hydrocarbon - Gasoline). Portland, Oregon: ODEQ.

Parkin, T.B. 1987. Soil microsites as a source of denitrification variability. *Soil Sci. Soc. Am. J.* 51, no. 5: 1194-1199.

Parkin, T.B., and J.A. Robinson. 1992. Analysis of lognormal data. *Advances in Soil Science* 20, 193-236.

Phelps, T.J., E.M. Murphy, S.M. Pfiffner, and D.C. White. 1994. Comparison between geochemical and biological estimates of subsurface microbial activities. *Microbial Ecology* 28, no. 3: 335-349.

Reinhard, M., S. Shang, P.K. Kitanidis, E. Orwin, G.D. Hopkins, and C.A. Lebron. 1997. In situ BTEX biotransformation under enhanced nitrate- and sulfate-reducing conditions. *Environmental Science and Technology* 31, no. 1: 28-36.

Ronen, D., M. Magaritz, E. Almon, and A.J. Amiel. 1987. Anthropogenic anoxification ("eutrophication") of the water table region of a deep phreatic aquifer. *Water Resources Research* 23, no. 8: 1554-1560.

Smith, R.L., B.L. Howes, and J.H. Duff. 1991. Denitrification in nitrate-contaminated groundwater: Occurrence in steep vertical geochemical gradients. *Geochimica et Cosmochimica Acta* 55, no. 7: 1815-1825.

Smith, R.L., S.P. Garabedian, and M.H. Brooks. 1996. Comparison of denitrification activity measurements in groundwater using cores and natural-gradient tracer tests. *Environmental Science and Technology* 30, no. 12: 3448-3456.

Starr, R.C., and R.W. Gillham. 1989. Controls on denitrification in shallow unconfined aquifers. In *Contaminant Transport in Groundwater,* ed. H.E. Kobus and W. Kinzelbach, 51-56. Rotterdam, The Netherlands: A.A. Balkema.

Stumm, W., and J.J. Morgan. 1981. *Aquatic Chemistry: An Introduction Emphasizing Chemical Equilibria in Natural Waters,* 2nd ed. New York: Wiley Interscience.

Thorstenson, D.C., D.W. Fisher, and M.G. Croft. 1979. The geochemistry of the Fox Hills-Basal Hell Creek aquifer in southwestern North Dakota and northwestern South Dakota. *Water Resources Research* 15, no. 6: 1479-1498.

Thurman, E.M. 1985. *Organic Geochemistry of Natural Waters.* Dordrecht, The Netherlands: Martinus Nijhoff.

Tiedje, J.M. 1988. Ecology of denitrification and dissimilatory nitrate reduction to ammonium. In *Biology of Anaerobic Microorganisms,* ed. A.J.B. Zehnder, 179-244. New York: John Wiley.

Trudell, M.R., R.W. Gillham, and J.A. Cherry. 1986. An in situ study of the occurrence and rate of denitrification in a shallow unconfined sand aquifer. *Journal of Hydrology* 83, no. 3/4: 251-268.

United States Environmental Protection Agency (U.S. EPA). 1986. Test methods for evaluating solid waste: Physical/chemical methods, 3rd ed. EPA 530/SW-846. Washington, D.C.: U.S. EPA Office of Solid Waste and Emergency Response.

Wilson, J.T., J.F. McNabb, D.L. Balkwill, and W.C. Ghiorse. 1983. Enumeration and characterization of bacteria indigenous to a shallow water-table aquifer. *Ground Water* 21, no. 2: 134-142.

Yoshinari, T., and R. Knowles. 1976. Acetylene inhibition of nitrous oxide reduction by denitrifying bacteria. *Biochemical and Biophysical Research Communications* 69, no. 3: 705-710.